Optics and Laser Technology 105 (2018) 15–22

Contents lists available at ScienceDirect

Optics and Laser Technology

journal homepage: www.elsevier.com/locate/optlastec

Full length article

Analysis on welding characteristics of ultrasonic assisted laser welding of AZ31B magnesium alloy

Zhenglong Lei [a,*], Jiang Bi [a], Peng Li [a], Tao Guo [a], Yaobang Zhao [b], Dengming Zhang [b]

[a] State Key Laboratory of Advanced Welding and Joining, Harbin Institute of Technology, Harbin 150001, China
[b] Shanghai Spaceflight Precision Machinery Institute, Shanghai 201600, China

ARTICLE INFO

Article history:
Received 7 September 2017
Received in revised form 4 February 2018
Accepted 23 February 2018

Keywords:
AZ31B Mg alloy
Laser welding
Ultrasonic vibration
Weld porosity
Microstructure
Mechanical properties

ABSTRACT

To the problems of welding porosity and poor weld formability in the laser welding process of magnesium (Mg) alloy, the experimental research of ultrasonic assisted laser welding of AZ31B Mg alloy was carried out, and its welding characteristics and the effect of ultrasonic vibration on microstructure and mechanical property of weld joint were analyzed. The results indicate that, the cavitation and acoustic streaming of ultrasonic vibration on weld pool can significantly improve weld defect and microstructure morphologies. With ultrasonic assisted laser welding technology, the weld appearance becomes smooth and sound. The weld porosity declines from 4.3% to 0.9% and its average size decreases. The width of columnar grain zone near fusion line decreases and the equiaxed grains in fusion center zone increase tremendously, the refining effect on the grain is obvious. Also, the mechanical properties of welds can be significantly improved, the tensile strength and elongation can be increased to 87% and 64% of the base metal.

1. Introduction

As light structure materials, Mg alloy has a low density and a high specific strength. Mg alloy is widely used in aerospace, automobile and mechano-electronic industry due to its enticing properties such as excellent mechanical damping property, electron shielding characteristic, welding and machining properties, recirculation and biodegradation properties [1]. The use of Mg alloys for typical automobile body parts can provide a mass reduction compared to current steel and aluminum construction, so as to reduce energy consumption [2]. In the biomedical field, based on its elastic modulus is similar to human skeleton and good biocompatibility, Mg alloy is an ideal material for surgical implants [3]. Therefore, Mg alloy is considered as “the greatest potential green engineering material of the 21st century”. And a feasible method for plastic processing in Mg alloy is sought, making it a hot issue in current engineering community.

In the application of Mg alloys in the automotive and aircraft industries, welding and joining would inevitably be involved. A variety of welding and joining techniques have been used to join Mg alloys friction stir welding (FSW), electron beam welding (EBW), tungsten-inert gas welding (TIG), metal-arc inert welding, CO_2 laser welding, and solid-state Nd:YAG laser welding. Luo et al. [4] joined AZ91D and ZG61 with FSW technology and indicated that the microhardness and tensile strength of ZG61/AZ91D joints are much larger than AZ91D/ZG61 joints. Fine-grain strengthening and texture strengthening are two main strengthening mechanisms. Chi et al. [5] studied the EBW technology of AZ series (AZ31B, AZ61A and AZ91D) Mg alloys and found that, with the increasing of Al content, the precipitated phases (β phase, $Mg_{17}Al_{12}$) is increased, its strength and hardness increase and the plasticity decreases, the fracture mode is changed from an irregular FZ fracture to a regular HAZ fracture. Sun et al. [6] evaluated TIG, CO_2, and pulsed Nd:YAG laser-welded joints of AZ31 sheet and reported that TIG welding could be used to achieve welds without defects, but they noted that coarser grain sizes in TIG welds could reduce the mechanical properties. For the laser welding has a series of advantages, such as high welding speed, precise control of power output, narrow joints with reduced heat affected zone (HAZ), low distortion and excellent environment adaptability, laser welding has been considered as a more potential processing method in the modern welding techniques of Mg alloys [7,8]. For example, Wahaba et al. [9] studied keyhole stability and porosity mechanism in laser welding of AZ series Mg alloys. Padmanaban et al. [10] studied the fatigue behavior of CO_2 laser welded AZ31 Mg alloy. Scintilla et al. [11] investigated the mechanical properties of Nd:YAG laser welded AZ31 Mg alloy. As a new kind of laser with

* Corresponding author.
E-mail address: leizhenglong@hit.edu.cn (Z. Lei).

https://doi.org/10.1016/j.optlastec.2018.02.050
0030-3992/

increased power density, good beam quality, and higher efficiency compared to equivalent power Nd:YAG lasers [12], fiber laser was recommended to join Mg alloys, which showed the tensile strength of welded joints could be stronger than base metal [13]. However, the metallurgical defects such as weld porosity and undercut also occurred easily in fiber laser welds of AZ31 [14], AMCa403 [15], AE42 and AS41 [16] Mg alloys. To some extent, the laser energy density is so high that the heat input pre unit area is large, so that it is easy to lead to grain coarsening. At the same time, the welding joints of Mg alloy are easy to produce porosity defects which can decrease its comprehensive properties. All of these are the main reasons for the limitation of the application of fiber laser welding of Mg alloys.

Based on its unique cavitation and acoustic streaming, introducing ultrasonic into weld pool can refine grains and eliminate the weld porosity and inclusion defect. Therefore, ultrasonic assisted welding technology is becoming the main research direction of Mg alloy laser welding. Xu et al. [17] developed the ultrasonic assisted tungsten inert gas welding-brazing technology and found that, with ultrasonic power of 1.2 kW, the morphology of columnar α-Mg grains was refined to approximately equiaxed grains, the average grain size of columnar grains decreased from 200 μm to 50 μm and the maximum joint strength of joints increased by 18.1%. Yuan et al. [18] studied the arc welding of Mg alloys (AZ31 Mg and AZ91 Mg) and found that effective grain refining can be achieved in welding by ultrasonic stirring of the weld pool with a probe positioned behind the arc.

In this paper, the AZ31B Mg alloy sheet is selected as the research object. The ultrasonic assisted laser welding process experiment is done to analysis the influence rule of technological parameters on welded joint mechanical property and microstructure. Based on this point, the ultrasonic assisted laser welding process program is designed. The material property testing and process test are combined to verify the feasibility of process program. The obtained results are expected to provide a new means and experimental basis on welding and joining of Mg alloy material.

2. Experimental methods and material

Commercially available AZ31B Mg alloy sheet with the dimension of 100 mm × 60 mm × 3 mm were used as specimens for ultrasonic vibration-assisted laser welding. The chemical composition of the base metal is listed in Table 1, which was measured by the PW4400 type X-ray fluorescence spectrometer with the measurement error less than 0.3 %.

Before welding, any oxide layer was removed from the surfaces by mechanical methods. And the specimens were cleaned with acetone, ethanol, and then dried. The laser beam welding was performed with a diffusion cooling carbon dioxide laser of 3.0 kW rated power (ROFIN-SINARDC030). The ultrasonic power supply (CSHJ-1000) delivered the power output of 800 W at a fixed frequency of 40 kHz. The ultrasonic amplitude is 6 μm. In the ultrasonic assisted welding process, only the AZ31B sheet metal moves. Other components (laser head and amplitude transformer) remain stationary. The sheet is fixed on the walking mechanism controller. And the walking mechanism controller, which is controlled by stepping motor, is designed by our research group. The main experimental apparatus is shown in Fig. 1.

Table 1
Chemical composition of the base metal (wt.%).

Al	Zn	Mn	Si	Ca	Cu	Mg
3.2	1.2	0.8	0.07	0.04	0.01	Bal

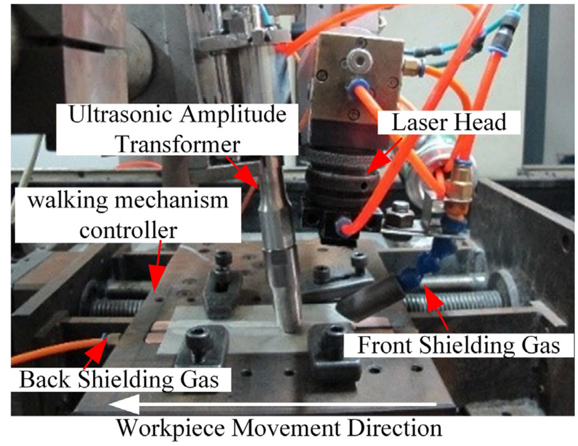

Fig. 1. The test equipment of ultrasonic vibration-assisted laser welding.

The ultrasonic is applied with the method of synchronized motion with the laser beam and it is delivered to the workpiece surface by amplitude transformer, the technological parameters are shown in Table 2. In order to prevent oxidation, argon was selected as, both, front and back shielding gas, with a gas flow rate of 15 l min^{-1} and 5 l min^{-1}, respectively. In the welding process, laser beam defects 5–10° to prevent reflected laser from damaging optical elements, such as the focus lens and the collimating lens.

The clamping force, F, can be calculated indirectly according to the cylinder diameter and compressed air pressure (P = 0.05, 0.1, 0.15, 0.2 MPa), the formula is as follows:

$$F = \frac{1}{4}\pi d^2 \cdot P \tag{1}$$

where the F is the amplitude transformer pressure on welding test plate, the d is the cylinder diameter and the P is the compressed air pressure.

The size of axial tensile specimen is determined by the international standard (ISO 6892: 1998) of the tensile specimen and the accuracy of experimental equipment (see Fig. 2). The tensile specimens are perpendicular to the weld direction. All the testing results were the average of three specimens. After laser welding, metallographic samples of the welded sheets were sectioned and then ground with sand papers. The metallographic etchant (10 ml acetic acid, 6 g picric acid, 10 ml water and 100 ml absolute ethyl alcohol) was used for chemical etching of the metallographic samples. Three different specimens were taken for each microstructural examination methods and the corrosion time is 5 s. Microstructural examination was conducted with an optical microscopy (OM, VHX-1000) and a scanning electron microscopy (SEM, Hitachi S-3400).

The microstructure of the base metal is shown in Fig. 3. The main elements of AZ31B Mg alloy are Mg and Al, which can form into solid solution. Also, the mechanical properties and corrosion resistance are all enhanced by the solution strengthening effect [19]. The grain sizes are 10–40 μm. The microstructure of original tube is equiaxed grain rather than fibrous structure because recovery and recrystallization occur in the preparation process. In order to identify the phase constitution, X-ray diffraction test is performed on the specimen cut from the base metal. Fig. 4 shows that the diffractive peaks of α-Mg and β-$Mg_{17}Al_{12}$ phase could be observed, and the β-$Mg_{17}Al_{12}$ is very few. That is because the maximum solubility of Al can reach up 12.7% in α-Mg matrix. And the solubility of Al decreases gradually with the temperature decreases. At the temperature of 150 °C, the solubility of Al decreases to 3%. However, the content of Al in AZ31B Mg alloy is